NEW PARAMETERS IN SHEAR WAVE ELASTOGRAPHY *IN VIVO*.

Jean-Luc Gennisson, Institut Langevin – Ondes et Images, 1 Rue Jussieu, 75005, Paris, France. Téléphone: 01 80 96 30 79, Adresse électronique: jl.gennisson@espci.fr.

Keywords: Ultrasound elastography, shear waves, viscoelasticity, anisotropy, elastic non linearity.

1. INTRODUCTION

Ultrasonography is a widely used medical imaging technique with many clinical applications. Used in clinical practice for more than 40 years, it is highly regarded for its ease of use, real-time capability, portability and low cost. Based on the propagation of mechanical waves and more particularly on high frequency compressional waves aka ultrasound, it allows the construction of morphological images of organs, but lacks a fundamental and quantitative information on tissue elastic properties; indeed the bulk modulus that governs the propagation of ultrasound is almost homogeneous in the different biological tissues and does not depend on tissue elasticity (Sarvazyan et al., 1995). Elastography, whose development started about 20 years ago, aims at imaging tissue stiffness, which provides an additional and clinically relevant information. Mapping the stiffness can either be estimated from the analysis of the strain in the tissue under a stress (quasi-static methods), or by the imaging of shear waves, mechanical waves, whose propagation is governed by the tissue stiffness rather than by its bulk modulus.

From a physics point of view, elastography aims to quantitatively image the Young's modulus, the physical parameter corresponding to the stiffness. This has two important advantages: the Young's modulus, noted *E*, exhibits important variations between different biological tissues, which makes it ideal for the characterization of different tissues with an excellent contrast (Sarvazyan et al., 1995); the Young's modulus characterizes the stiffness of a tissue, which is exactly the quantitative reproduction of a clinician's palpation and has relevant diagnostic value. This simple and intuitive relationship between palpation and elastography calls for many applications of this ''palpation imaging'' such as breast tumor characterization and hepatic fibrosis staging where it was successfully been validated.

Wherever palpation has been shown to have a clinical value, elastography can be seen as a relevant tool for diagnosis. Moreover, although palpation requires a direct contact and can only be applied to superficial organs, many elastography techniques can also be applied to deep organs opening new possibilities of diagnosis. To assess the Young's modulus of the tissue, all elastography techniques rely on the same basis: an external force is applied to the studied tissue and the resulting movements are then followed. The external force can be classified according to two means of excitation: the static methods (or the quasi-static method) and the dynamic methods.

In the field of shear wave elastography, a specific technique called Supersonic Shear Imaging (SSI) was developed since almost fifteen years. This technique is based on two concepts: By means of the acoustic radiation pressure phenomena shear waves are generated directly within tissues. Then shear wave propagation is caught in real time by using an ultrafast ultrasound device (up to 20000 frames/s). As shear wave speed is directly related to stiffness of tissues, such a concept allows to recover elastic maps of organs. Nevertheless stiffness is not always only sufficient to better understand organs pathologies and behaviors. So there is a need to add new parameters for a better characterization. In this context, SSI technique can be extended in order to reach new mechanical parameters which can potentially help physicians. By looking at the shear wave dispersion, viscosity of tissues can be retrieved by using the right rheological model. Elastic anisotropy is recovered by rotating the probe at the surface of the investigated organ. For each position, the shear wave speed is calculated allowing to deduce orientation of fibers. At last, the change in tissue stiffness as a function of the pressure applied over medium, also called acoustoelasticity theory, allows the assessment of the nonlinear elastic properties. The combination of all these new parameters, viscosity, anisotropy and nonlinearity,

with stiffness offer new possibilities of diagnosis for physicians to better understand organs pathologies.

2. SUPERSONIC SHEAR IMAGING

The Supersonic Shear Imaging technique is the outcome of researches at the Institute Langevin in transient elastography. The idea of combining radiation pressure or acoustic radiation force and the study of shear waves generated comes from Armen Sarvazyan, which can be considered as a precursor of elastography techniques based on ultrasonic radiation pressure via its technique: Shear Wave Elasticity Imaging (Sarvazyan et al., 1998). In 2004, two fundamental ideas are developed to overcome the limitations of 2D elastography technique: first acoustic radiation force and second ultrasound ultrafast imaging. These two concepts described below are at the heart of the Supersonic Shear Imaging technique (Bercoff et al., 2004a) (Fig. 1):

• A Mach cone: ultrasound beams are successively focused at different depths. The different spherical waves generated for each focal beam interfere like a Mach cone (Bercoff et al., 2004b) in which the source propagates more quickly than the generated shear wave and creates a quasi-plane wave front in the imaging plane (cylindrical in three dimensions). The use of constructive interfaces makes it possible to increase the amplitude of the wave and thus the signal to noise ratio of the displacement field. The generated quasi-plane shear wave in the imaging plane allows also simplifying the propagation hypotheses, which is of great interesting to solve inverse problems. Finally, only one Mach cone allows illuminating almost all of the medium with one plane shear wave; shear wave being generated, the propagation equation of the waves is inverted to rebuild a map of Young's modulus;

• Ultrafast imaging: complete acquisition all at once. Ultrafast imaging allows scanning the entire imaging plane with very good temporal resolution in one single acquisition, typically with a frame rate of 5000 images per second, and up to 30,000 images per second in the case of tissues such as the peripheral arteries or the eye. Therefore there is no need to repeat the acquisition several times by stroboscopy to acquire the entire displacement field. This allows, not only imaging in real-time, which makes the examination easier, but also averaging the very rapidly acquired images to improve image quality.

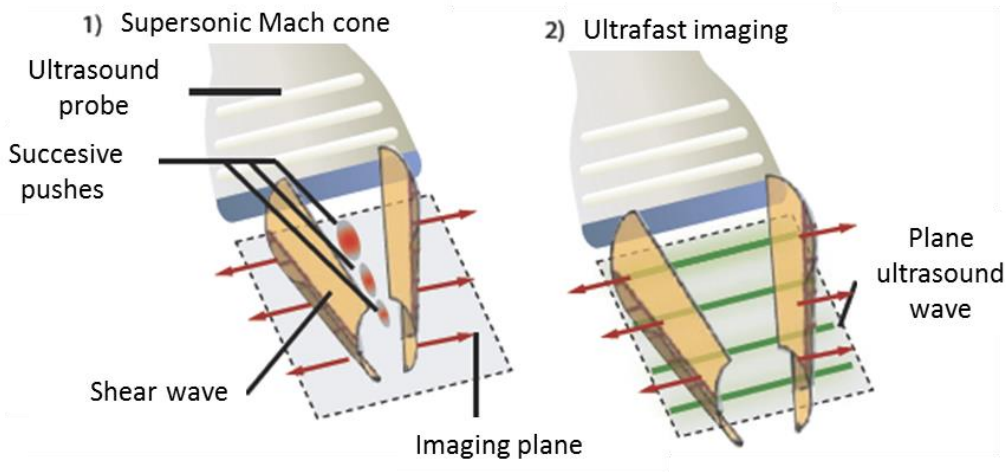

Figure 1 : 1: the ultrasounds are successively focused at different depths to create pushes by radiation pressure. The constructive interferences of the shear waves form a supersonic Mach cone (in which the speed of the source is greater than the speed of the generated wave) and a quasi-plane shear wave is created; 2: the ultrasound machine then switch into an ultrafast imaging mode to follow the shear wave that is propagating through the medium.

Therefore, the Supersonic Shear Imaging technique uses the technology of the 2D transient elastography, but substitute's vibrator by the acoustic radiation pressure. The whole excitation-imaging method is then integrated onto one single component: the ultrasound imaging transducer array. Amplified by the Mach cone, the generated shear wave has amplitude of tens of microns. This latter is detectable with a good signal to noise ratio by ultrasound speckle tracking algorithm and ultrafast imaging. Thanks to ultrafast imaging, the acquisition of the shear wave propagation can be carried out all at once in less than 30 milliseconds. The technique is therefore slightly sensitive to patient movements (as an example breathing) and can be displayed in real-time, like a conventional ultrasound image. The Young's modulus maps are then reconstructed by estimating the speed of the shear wave between two points of the image, using a time of flight algorithm. The first *in vivo* experiences with this technique were conducted at the Institut Curie where, in 50 patients, the use of the technique to differentiate benign tissue from malignant tissue was demonstrated (Tanter et al., 2008) (Fig. 2).

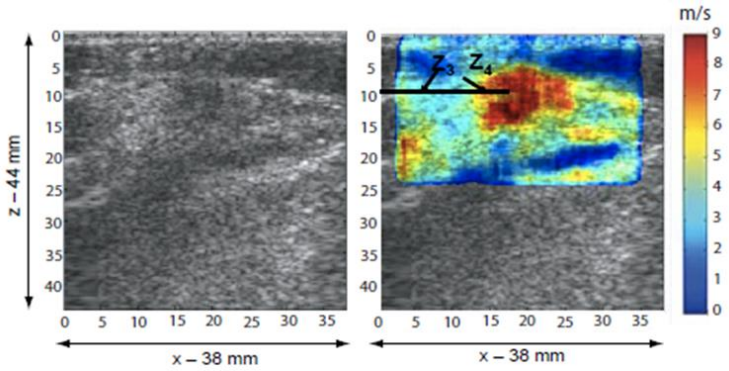

Figure 2 : Ductal infiltrating carcinoma. The B-mode image brings out a hypo-echogenic mass with blurry borders with a shadow posterior to the lesion. The lesion is classified as ACR5. The elasticity imaging clearly brings out a very stiff mass at more than 150 kPa (7.1 m/s) (Tanter et al., 2008).

This technique was implemented on an ultrasound diagnostic imaging device called, the Aixplorer® (Supersonic Imagine, Aix-en-Provence, France) and its diagnosis performance as well as its reproducibility were demonstrated in several organs, and more particularly in the breast (Cosgrove et al., 2011). In particular, a multicentric study in 939 patients with breast cancer showed an important increase in specificity for breast lesion characterization (+17.4%) with the addition of the elasticity parameters to the classical BIRADs criteria (Berg et al., 2012). However, in terms of mechanical behavior, biological soft tissues are much more complex and elasticity could not be enough to perfectly describe media and potentially improve physician diagnosis in other organs. In that way the technique was enhanced in order to asses other mechanical parameters such as elastic anisotropy, viscosity and elastic non linearity.

3. ANISOTROPY

The muscle model considered in this paper presents a random distribution of fibers oriented in the same direction. This consideration entails the existence of a symmetry axis along the fibers. It is proven that this kind of symmetry corresponds to a hexagonal system (transverse isotropy) (Zimmer et al., 1970). The Christoffel's matrix c_{ijkl} of such a system contains 5 independent elastic constants. The eigenvectors of the Christoffel's tensor are associated to eigenvalues which are the speeds of waves in all directions. Nevertheless, we are only interested in wave propagation along the axis perpendicular to the muscle fibers since the direction parallel to the fibers is not easily accessible *in vivo* for the specific setup considered in this analysis. Moreover the weak backscattered signal for an ultrasonic beam parallel to this latter direction makes the use of transient elastography difficult. Therefore, in the direction perpendicular to the fibers the speeds of the three different waves are for the shear wave with a polarization perpendicular to the fibers ($V_{S\perp}$) and for the shear wave with a polarization parallel to the fibers

($V_{S//}$) respectively: $c_{44} = \rho.V_{S//}^2$ and $c_{66} = \rho.V_{S\perp}^2$, where ρ is the density. It clearly appears that the elastic moduli c_{44} and c_{66} can be obtained if one is able to measure the speed of polarized shear waves. Using these techniques, for each orientation of the probe compared to the main axis of the muscle fibers (in the following, along the fibers is notified by the symbol // and perpendicularly is notified by the symbol $\perp$) two experiments were tested: The influence of loading on the elasticity of the muscle in terms of global elasticity and the elastic anisotropic properties of the brachialis muscle.

Mapping of shear wave group velocity during isometric contraction

The first experiment was made for different loads (from T 5 0 kg to 5 kg with 1 kg step). Elasticity maps were acquired for two different axis of insonification in the muscle, along the fibers (Fig. 3) and perpendicularly to the fibers (Fig. 4). An increase of the global elasticity of both muscles is clearly visible in both configurations (from 4.0 to 36.6 kPa // and from 2.3 to 4.0 kPa t in shear modulus under the assumption of a purely elastic model). Moreover, the elasticity contrast between the biceps and the brachialis increases strongly with contraction when measured along the fibers (Fig. 3) but gently when measured perpendicularly to the fibers (Fig. 4). Biceps and brachialis muscles can, thus, be separated in terms of the change in elasticity with the contraction. With no contraction, the biceps brachii, softer than the brachialis when measured along the fibers, is harder than the brachialis when measured perpendicularly to the fibers.

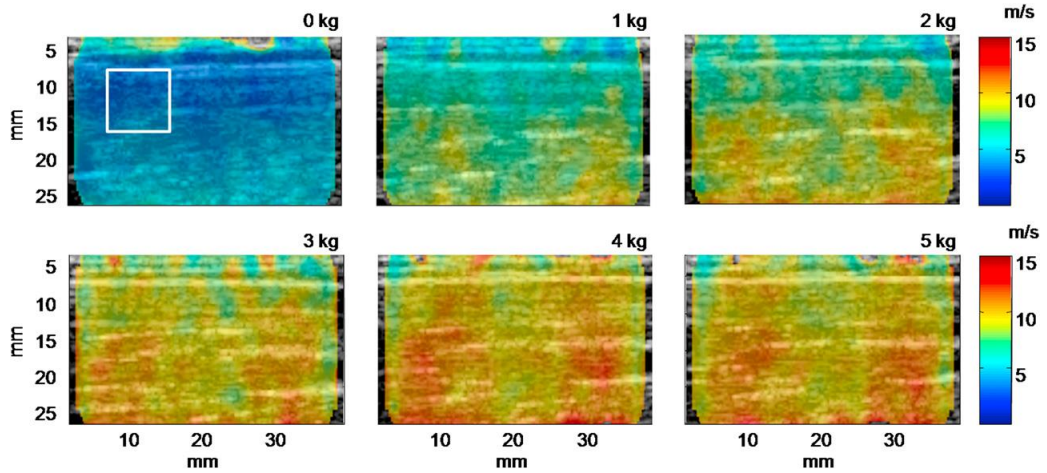

Figure 3 : Shear velocity maps of the biceps brachii and brachialis muscles as a function of the load from T 5 0 to 5 kg along the fiber // (longitudinal). Volunteer was placed in prone position with a 90° angle of the elbow (Gennisson et al., 2010).

Shear wave group velocity and anisotropy

Anisotropic properties measured on a volunteer are shown in Figure 5 where shear wave group velocity is plotted as a function of the angle between the probe and the main axis of the muscle fibers for two different loads (0 kg and 3 kg). For 0°, corresponding to a propagation of the shear wave along the fibers, the shear wave group velocity is three times higher for a 3 kg loading than at rest. For 90°, corresponding to a propagation of the shear wave perpendicularly to the muscle fibers, the shear wave group velocity is barely higher at rest than for a 3 kg loading. In between those two main axes (0° and 90°) the shear wave group velocity increase for both loads, result that is in good agreement with the literature (Gennisson et al. 2003). However, one can notice that anisotropy is more visible in the contracted state that in the rest state. Each intermediate position of the probe corresponds to a mix of the elastic properties parallel and perpendicular to the fibers.

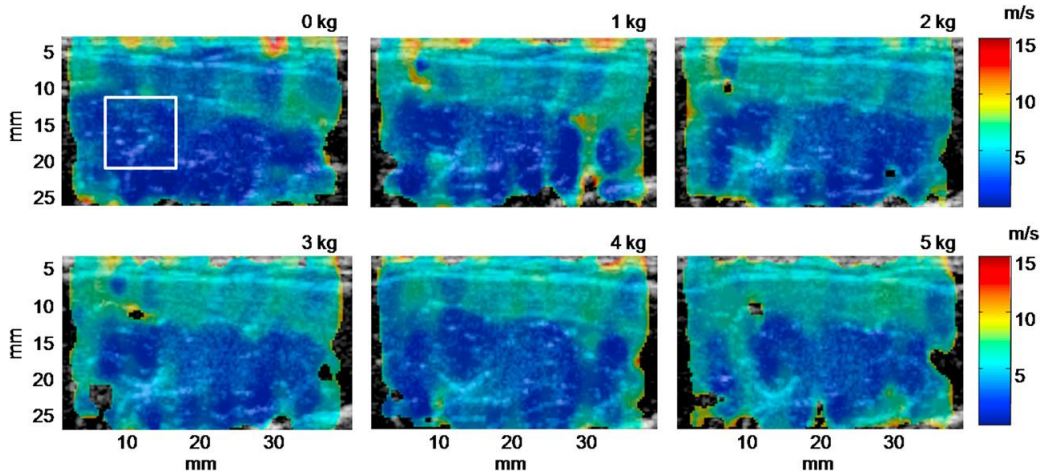

Figure 4 : Shear velocity maps of the biceps brachii and brachialis as a function of the load from T 5 0 to 5 kg measured perpendicularly to the fibers (transverse). Volunteer is placed in prone position with a 90° angle of the elbow. The two muscles biceps brachii (the biceps [upper part], the brachialis [lower part]) are easily distinguishable in terms of shear wave speed (Gennisson et al., 2010).

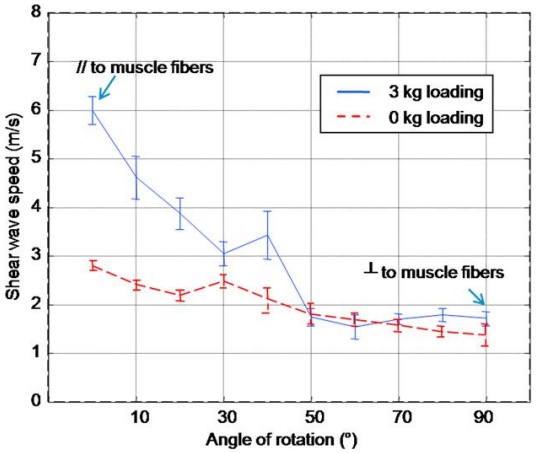

Figure 5 : Shear wave group velocity as a function of the angle of rotation q between the ultrasonic probe and the muscle fibers. q 5 90_ corresponds to the probe perpendicularly to the fibers and q 5 0_ corresponds to the probe placed along the fibers. Two levels of contraction are presented T 5 0 kg (blue solid curve) and T 5 3 kg (red dashed curve). The errorbars correspond to the standard deviation over the whole elastic map for each angle of rotation (Gennisson et al., 2010).

4. VISCOSITY

Non-invasive evaluation of rheological behavior of soft tissues may provide an important diagnosis tool. Nowadays, available commercial ultrasound systems only provide shear elasticity estimation by shear wave speed assessment under hypothesis of a purely elastic model. However, to fully characterize the rheological behavior of tissues, through storage (*G'*) and loss (*G"*) moduli, it is necessary to estimate also shear wave attenuation. Shear waves generated in the SSI technique are not plane. When using SSI the wave amplitude observed in a plane decreases not only by action of medium absorption but also by diffraction effect. This generates the need of a correction when attempting to use attenuation coefficient to characterize the rheological behaviour of the medium. Consequently, a diffraction correction is needed to estimate the shear wave attenuation. The use of a cylindrical wave approximation to take into account diffraction was already proposed. In this work the use of a cylindrical wave

approximation proposed by different authors (Deffieux et al., 2009; Nenadic et al., 2014) is revisited experimentally and through numerical simulation in order to verify its validity. Afterwards maps of *G'* and *G''* for an isotropic and homogeneous viscoelastic medium were calculated. Figure 6, G' and G'' maps calculated at 300 Hz images for a two layered phantom. The left layer is a 5% gelatin – 2% agar gel while the right layer is a 5% gelatin – 2% agar phantom with 10% glycerol addition. The phantom was made in order to have the same value in shear wave velocity and two layer in shear wave attenuation. Knowing G' and G" allows to characterize any rheological model.

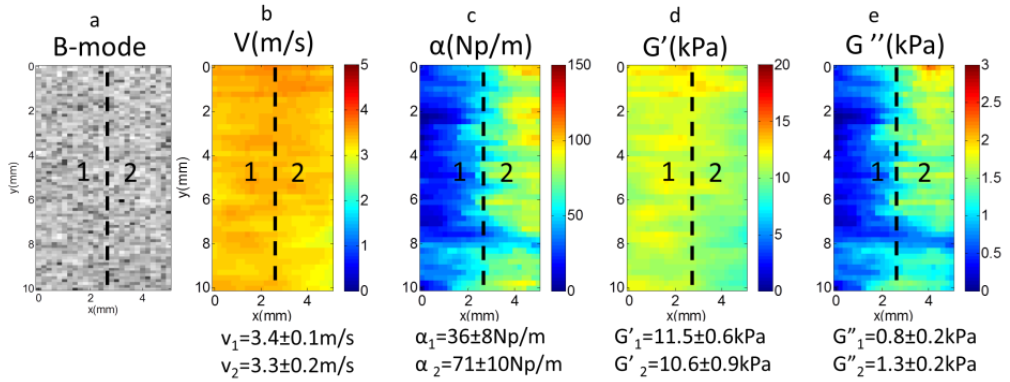

Figure 6 : a) Bmode, b) Shear wave velocity, c) shear wave attenuation, d) storage modulus, e) loss modulus for the two layered phantom. The dashed line indicates the boundary between the two layers. Left layer 0% glycerol – Right layer 10% glycerol.

5. ELASTIC NON LINEARITY

Breast cancer detection in the early stages is of great importance since the prognosis and the treatment greatly depend on this. Multiples techniques relying on the mechanical properties of soft tissues have been developed in order to help in the early detection. In this study we implemented a technique that measures the nonlinear shear modulus (NLSM) (μ_{NL}) *in vivo* and showed its utility to detect breast lesions from healthy tissue. The technique relies on the acoustoelasticity theory in quasi-incompressible media. In order to recover μ_{NL}, static elastography and supersonic shear imaging are combined to subsequently register strain maps and shear modulus maps while the medium is compressed. The combination of both techniques allow to recover the stress map within the medium.

The acoustoelasticity theory is based on the effect of uniaxial or hydrostatic pressure on the speed of waves. In an isotropic and homogeneous material where the axis of the uniaxial compression is parallel to the shear wave polarization and in which a plane shear wave of low amplitude propagates, the wave equation derived is:

$$\rho \frac{\partial^2 u_z^D}{\partial t^2} = \frac{\partial^2 u_x^D}{\partial z^2}\left[\mu + 2\mu\left(\frac{\partial u_x^S}{\partial x} + 2\frac{\partial u_z^S}{\partial z}\right) + \frac{A}{2}\left(\frac{\partial u_x^S}{\partial x} + \frac{\partial u_z^S}{\partial z}\right)\right] , \quad (1)$$

where $u^D_{x,z}$ and $u^S_{x,z}$ are displacements due to the shear wave and static uniaxial stress (σ_z) respectively (Gennisson et al., 2007). In the case of shear wave displacements smaller than static compression and by applying the Hooke's law, the nonlinear elastodynamic equation is rewritten as:

$$\rho V_s^2 = \mu_0 - \sigma_z\left(\frac{A}{12\mu_0}\right), \quad (2)$$

with μ_0 being the shear modulus at stress free condition.

Then by quantifying the shear wave speed as a function of the stress applied one can recover the nonlinear shear modulus *A* (third order Landau coefficient). Thereafter, as it is very

difficult to apply an uniaxial stress experimentally, one cannot use A as the definition of the quantified NLSM since it is defined for an uniaxial stress. Then the NLSM is denoted as μ_{NL} and is closely related to A. *In vivo*, the breast was compressed manually by a trained radiologist using the ultrasound probe fitted with a plastic plate allowing a more uniform deformation. Since the pressure was applied uniaxially in all the cases, all the deformations were assumed to be positive.

During experiments, number of compressions was 6. The sampling rate of the ultrafast sequence was set to 100 Hz and 100 images were acquired between consecutive compressions. Such acquisitions allow to compute strain maps and combined with SSI to calculate stress maps. At the beginning of the experiment, patients were positioned in the supine position, slightly tilted depending on the location of the mass. The overall experiment for each patient was performed in less than 30 s. Figure 7 shows the results of the NLSM for one healthy subject (first row), a patient with a tumor (carcinoma, middle row) and a patient with a benign lesion (fibroadenoma, bottom row). Panels a, d and g show the ultrasound images registered during the clinical exam for all 3 subjects. The masses are encased in a red box (--·--) and highlighted with a white arrow. Panels' b, e and h show the corresponding shear elasticity maps. Panels' c, f, I show the corresponding μ_{NL} maps.

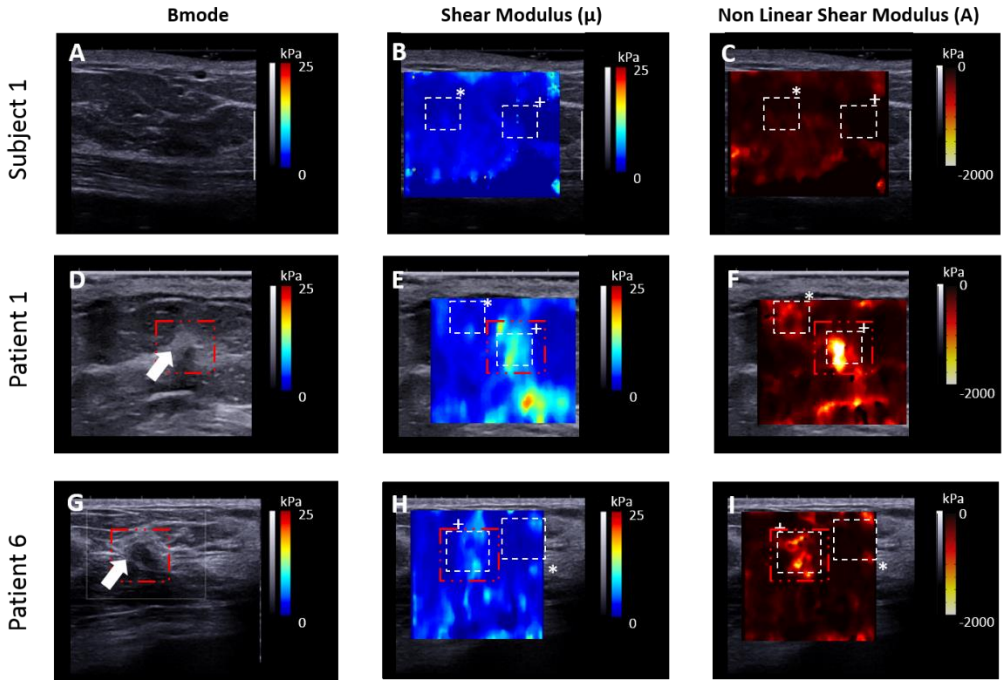

Figure 7: Results of the NLSM on 3 patients, a healthy volunteer, a patients presenting with a tumor and a patient with a benign lesion. The left column shows the ultrasound images where the mass are enclosed in red squares. The center and the right columns show the corresponding images for the shear and the nonlinear shear modulus, respectively. The dotted squares are the ROI's used in the mean and standard deviation values (Bernal et al., 2016).

6. CONCLUSION

The combination of all these new parameters, viscosity, anisotropy and nonlinearity, with stiffness offer new possibilities of diagnosis for physicians to better understand organs pathologies.

REFERENCES

Bercoff J, Tanter M, Fink M. “Supersonic shear imaging: a new technique for soft tissue elasticity mapping.”, *IEEE Trans Ultrason Ferroelectr Freq Control*, **51**, 4, (2004a), pp. 396-409.

Bercoff J, Tanter M, Fink M. “Sonic boom in soft materials: the elastic Cerenkov effect”, *Appl Phys Lett*, **84**, 12, (2004b), pp. 2202-2204.

Berg WA, Cosgrove DO, Doré CJ, et al. “Shear-wave elastography improves the specificity of breast US: the BE1 Multinational Study of 939 Masses.” *Radiology*, **262**, 2, (2012), pp. 435-449.

Bernal M, Chamming’s F, Couade M, Bercoff J, Tanter M, Gennisson JL, “In vivo quantification of the nonlinear shear modulus in breast lesions: feasibility study.”, *IEEE Trans Ultrason Ferroelectr Freq Control*, (2016), in press.

Cosgrove DO, Berg WA, Doré CJ, et al. “Shear wave elastography for breast masses is highly reproducible.”, *Eur Radiol*, , (2011).

Deffieux T., Montaldo G., Tanter M., and Fink M. “Shear Wave Spectroscopy for In Vivo Quantification of Human Soft Tissues Visco-Elasticity.” *IEEE Trans on Medical Imaging*, **28**, 3, (2009).

Gennisson JL, Catheline S, Chaffaı¨ S, Fink M. “Transient elastography in anisotropic medium: Application to the measurement of slow and fast shear waves velocities in muscles.” *J Acoust Soc Am*, **114**, (2003), pp.536–541.

Gennisson J.L., Deffieux T, Macé E, Montaldo G, Fink M., Tanter M. “Viscoelastic and anisotropic mechanical properties of in vivo muscle tissue assessed by Supersonic Shear Imaging.” *Ultr. Med. & Bio.*, **36**, 5, (2010), pp.789-801.

Gennisson JL, Rénier M, Catheline S, Barrière C, Bercoff J, Tanter M, Fink M. “Acoustoelasticity in soft solids: assessment of the nonlinear shear modulus with the acoustic radiation force.” *J. Acoust. Soc. Am.*, **122**, 6, (2007), pp.3211-3219.

Nenadic I., Urban M., Zhao H., Sanchez W., Morgan P., Greenleaf J. and Chen S. “Application of Attenuation Measuring Ultrasound Shearwave Elastography in 8 Post-Transplant Liver Patients”. *IEEE International Ultrasonics Symposium Proceedings*, (2014).

Sarvazyan A, Skovoroda AR, Emelianov S, Fowlkes JB. “Biophysical bases of elasticity imaging.” *Acoust Imag*, **21**, (1995), pp. 223-241.

Sarvazyan A, Rudenko O, Swanson S, Fowlkes J. “Shear wave elasticity imaging: a new ultrasonic technology of medical diagnostics.” *Ultrasound Med Biol* **24**, 9, (1998), pp.1419-1435.

Tanter M, Bercoff J, Athanasiou A, Deffieux T, Gennisson JL, Montaldo G, et al. “Quantitative assessment of breast lesions viscoelasticity using supersonic shear imaging.”, *Ultr Med Bio*, (2008).

Zimmer J., Cost J., “Determination of the elastic constants of an unidirectional fiber composite using ultrasonic velocity measurements” *J.Acoust. Soc. Am.* **47**, (1970), pp.795–803.